Robotica (2019) volume 37, pp. 675–690. © Cambridge University Press 2018
doi:10.1017/S026357471800125X

On the Maximization of Joint Velocities and Generalized Reactions in the Workspace and Singularity Analysis of Parallel Mechanisms

Pavel Laryushkin†, Victor Glazunov‡ and Ksenia Erastova†*

†Fundamentals of Machine Design Department, Bauman Moscow State Technical University, 2-ya Baumanskaya st. 5, Moscow 105005, Russia. E-mail: pav.and.lar@gmail.com
‡Mechanical Engineering Research Institute of the Russian Academy of Sciences (IMASH RAN), Maly Kharitonyevsky Pereulok 4, Moscow 101990, Russia. E-mail: vaglznv@mail.ru

(Accepted November 01, 2018. First published online: December 14, 2018)

SUMMARY
An approach for calculating the maximum possible absolute values of joint velocities or generalized reactions in a leg of a parallel mechanism has been considered in this paper. The Jacobian analysis and the Screw theory-based methods have been used to acquire the result. These values are calculated for the "worst" directions of the external load or end-effector's velocity for each leg. The feasibility of using these parameters as the measures of closeness to different types of parallel mechanism singularity is discussed. Further, how this approach is related to the state-of-the-art methods has been illustrated. The key aspect of the discussed approach is that the normalization of vectors or screws is carried out separately for angular and linear components. One possible advantage of such an approach is that it deals only with the kinematic and statics of the mechanism while still providing physically meaningful and practically applicable measures. Case studies of a 3-Degrees Of Freedom translational parallel mechanism and a planar parallel mechanism are presented for illustration and comparison.

KEYWORDS: Parallel mechanism; Workspace; Closeness to singularity; Singularity analysis; Screw theory; Jacobian.

1. Introduction

The existence of certain poses that are called "singular" is a significant problem for parallel mechanisms. In these poses, the kinematic or static properties of a mechanism change. It is also a well-known fact that the closeness to singular poses affects the performance of the mechanism.[1] Thus, it is important to study these singularities in order to properly design, build, and use these mechanisms.[2,3] Therefore, many researchers have focused their efforts on determining the singularity loci and poses,[4–6] planning trajectories that avoid such poses,[7–9] and calculating various "performance" indices.[10–16] Numerous different indices and parameters, such as the inverse condition number, the smallest singular value of a Jacobian matrix, pressure angles, etc., can be used to estimate how close the mechanism is to its singular pose. However, it is difficult to determine the admissible value for a transmission index from a practical point of view. The other problem that many of the proposed indices have is that they do not have a clear physical meaning.

* Corresponding author. E-mail: erastovakg@gmail.com

Depending on the singularity type,[17,18] a significant increase may be observed in the joint velocities or reactions when the mechanism's end-effector approaches the singular pose. Consequently, these two parameters can be used for calculating an "effective" workspace of robots, essentially excluding working areas where the mechanism is "too close" to the singular pose and the values of the velocities or reactions are too big. For instance, an algorithm for determining the border of the so-called "static workspace" was introduced in ref. [19]. This is a part of the workspace of the entire mechanism that includes all the points for which the maximal torques or forces in the legs of the mechanism do not exceed certain threshold values for a given external load. However, this analysis was done for a predefined external wrench. Thus, the "static workspace" will change its size or form if the direction of the external wrench is changed. Moreover, for many robot applications, the direction of the load wrench is not specified. Thus, this approach may require a significant amount of time to compute the values of the actuation efforts, since every possible direction (with a reasonable step) of the external load wrench should be taken into account.

In this paper, we discuss an approach for calculating the values of the generalized reactions (forces or torques) and velocities for a given norm of the external load or motion twist (or vector) of the end-effector, respectively. The key component of this approach is that it deals with the "worst" directions of the external load or motion of the end-effector that produce the generalized velocities with the maximum possible magnitude or maximize the generalized reactions (including the actuation velocities and efforts) in the mechanism's legs. The discussed approach will be illustrated using 3-Degrees Of Freedom (DOF) translational and planar parallel manipulators.

As for using the discussed approach to measure the closeness to the different types of singularities, we are mostly interested in how it is related to the work of Volgewede.[20,21] In these papers, a thorough analysis of the closeness to singularity measures was performed. However, the physically meaningful and practically applicable measures presented in his work require some non-kinematic properties of the mechanism (stiffness, inertia, etc.) to be introduced to the measure calculation (this was also noted by Merlet in his book[1]). A link between the discussed approach and the Voglewede's work on the topic will be illustrated in Section 4 of this paper.

We also make certain assumptions in order to simplify the explanations:

1. The number of DOFs of the end-effector in any non-singular pose is equal to the number of actuated joints.
2. Only one joint in each leg is actuated. Keeping the first assumption in mind, this also means that the number of legs is equal to the number of DOFs of the mechanism. Further, we also assume that all the actuated joints are located on the base plate of the mechanism. We begin enumerating joints within a leg starting from the actuated joint.
3. All kinematic pairs (joints) are 1-DOF, since any joint with a greater degree of freedom can be represented as a combination of 1-DOF joints.

Thus, in this paper, we consider an n-DOF parallel mechanism with n legs, with only the first joint being actuated in each leg. However, the approach can be extended to more complex cases, although this is beyond the scope of this paper. Furthermore, many of the widely used parallel mechanisms' topologies correspond to these assumptions.

In the next two sections, we describe the discussed approach using the Jacobian analysis and the Screw theory. The objective of this work is to study the basic fundamental properties of parallel mechanisms near the singularities. Therefore, performing the influence analysis of friction, damping, joint tolerances, etc., is beyond the scope of this paper.

2. Jacobian Analysis Approach

It is well known that, for any parallel mechanism, the relationship between its input (actuated) and output velocities can be expressed using the inverse Jacobian matrix $\mathbf{J}^{\text{inv}}$ of this mechanism (The matrix shown in this equation is called "inverse" because it defines the output-input velocity map. However, this definition may differ in different articles and books. The matrix can also be referred to as "actuation Jacobian," indicating that only the actuated ones of all joint velocities are considered):

$$\dot{\boldsymbol{\theta}} = \mathbf{J}^{\text{inv}} \cdot \dot{\mathbf{x}},$$

where $\dot{\boldsymbol{\theta}}$ and $\dot{\mathbf{x}}$ are the column vectors of the input and output velocities, respectively.

On the other hand, for the (column) vectors of actuation efforts $\mathbf{e}$ and external load $\mathbf{F}$, we can write the following:

$$\mathbf{e} = -\mathbf{J}^T \cdot \mathbf{F},$$

where $\mathbf{J}$ is the Jacobian matrix. It is to be noted that if the full-cycle mobility of the mechanism $\mathcal{M}$ is equal to its number of actuated joints N_a (which is true under the assumptions made in the previous section), then $\mathbf{J}^{\text{inv}}$ and $\mathbf{J}$ are square matrices, while for any non-singular configuration, $\mathbf{J}^{\text{inv}} = \mathbf{J}^{-1}$. Additionally, $\mathbf{F}$ here can act only on the directions that correspond to the allowed motions (all feasible $\dot{\mathbf{x}}$) of the mechanism.

As $\mathbf{J}^{\text{inv}}$ is constant for any particular mechanism configuration, it is quite clear that, in this case, for any given norm of $\dot{\mathbf{x}}$, the maximum possible absolute value of the velocity in the ith ($i = 1, \ldots, N_a$) actuated joint $|\dot{\theta}_i|^{\max}$ corresponds to the vector $\dot{\mathbf{x}} = \dot{\mathbf{x}}_i^{\max}$ collinear to the vector $\mathbf{j}_{\text{inv}i}$, which is the ith row of $\mathbf{J}^{\text{inv}}$. Further, this direction of $\dot{\mathbf{x}}$ need not be calculated, as $|\dot{\theta}_i|^{\max}$ is essentially a dot product of two vectors that fall on the same line:

$$\left|\dot{\theta}_i\right|^{\max} = \left\langle \mathbf{j}_{\text{inv}i}, \dot{\mathbf{x}}_i^{\max} \right\rangle = \left\|\mathbf{j}_{\text{inv}i}\right\| \cdot \|\dot{\mathbf{x}}\|, \tag{1}$$

where $\langle \cdot, \cdot \rangle$ denotes a dot product. Thus, if the norm of $\dot{\mathbf{x}}$ is given, then calculating $|\dot{\theta}_i|^{\max}$ is simple and straightforward because the components of $\mathbf{J}^{\text{inv}}$ can usually be obtained in a closed form as partial derivatives of the constraint equations.

Consequently, for the actuation effort in the ith active pair, we can write the following:

$$|e_i|^{\max} = \left\langle \mathbf{j}_{Ti}, \mathbf{F}_i^{\max} \right\rangle = \left\|\mathbf{j}_{Ti}\right\| \cdot \|\mathbf{F}\|, \tag{2}$$

where $|e_i|^{\max}$ is the maximum possible absolute value of the actuation effort on the ith actuated joint and $\mathbf{j}_{Ti}$ is the ith row (vector) of the transpose Jacobian matrix $\mathbf{J}^T$. Usually, the Jacobian matrix $\mathbf{J}$ can be computed only numerically as the inverse of $\mathbf{J}^{\text{inv}}$.

The major issue with this approach is that $\dot{\mathbf{x}}$ has to be normalized. This is a problem if the units of the components of $\dot{\mathbf{x}}$ are not consistent. Since $\dot{\mathbf{x}}$ may contain both angular and linear velocities, it is obvious that the Euclidean norm would not have clear physical significance in this case. In other words, the choice of norm has a huge impact on the physical interpretation of the results.

One possible solution to this problem is to consider the angular and linear components separately. Indeed, for a particular mechanism, we usually have requirements that would assign certain desired values to the end-effector's angular and linear velocities separately; these values may even be different for the velocities of the same type (for instance, the required speed of the end-effector may be higher for the xy-plane and lower for the z-axis). In this case, we can rewrite (1) as follows:

$$\left|\dot{\theta}_i\right|^{\max} = \left|\dot{\theta}_i\right|_{\omega}^{\max} + \left|\dot{\theta}_i\right|_{v}^{\max} = \left\|\mathbf{j}_{\text{inv}i}^{\omega}\right\| \cdot \|\boldsymbol{\omega}\| + \left\|\mathbf{j}_{\text{inv}i}^{v}\right\| \cdot \|\mathbf{v}\|. \tag{3}$$

Here, $|\dot{\theta}_i|_{\omega}^{\max}$ and $|\dot{\theta}_i|_{v}^{\max}$ are the maximum possible absolute values of the joint velocity in the ith actuated pair corresponding to angular ($\boldsymbol{\omega}$) and linear ($\mathbf{v}$) parts of vector $\dot{\mathbf{x}}$, respectively. Vectors $\mathbf{j}_{\text{inv}i}^{\omega}$ and $\mathbf{j}_{\text{inv}i}^{v}$ consist only of components of the ith row of $\mathbf{J}^{\text{inv}}$, which correspond to $\boldsymbol{\omega}$ and $\mathbf{v}$, respectively.

In a similar manner, for the actuation efforts, we can rewrite (2):

$$|e_i|^{\max} = |e_i|_f^{\max} + |e_i|_m^{\max} = \left\|\mathbf{j}_{Ti}^{f}\right\| \cdot \|\mathbf{f}\| + \left\|\mathbf{j}_{Ti}^{m}\right\| \cdot \|\mathbf{m}\|, \tag{4}$$

where vectors $\mathbf{j}_{Ti}^{f}$ and $\mathbf{j}_{Ti}^{m}$ consist only of components of the ith row of the $\mathbf{J}^T$ and correspond to external force ($\mathbf{f}$) and torque ($\mathbf{m}$), respectively.

It is to be noted that even if the full-cycle mobility is greater than the number of the end-effector DOFs (the mechanism has the so-called kinematic redundancy[22]), there will be no alteration to the approach, as all of the supplementary DOFs of the mechanism can also be considered separately. The case of the actuation redundancy[22] (Jacobian matrices are not square) is beyond the scope of this paper.

Although the maximum speed and force/torque of any actuation device will be specified, these parameters are not generally independent. Further, in practice, the maximum speed of a joint may depend on a number of factors, including loading and power input limit of the joint that may not be known. All these factors are not considered in the discussed approach, but some notes may be made

https://doi.org/10.1017/S026357471800125X Published online by Cambridge University Press

regarding its practical application. For example, it is possible to use the combination of velocity and effort in the actuated joint to compute the power required to execute a motion of the end-effector with the desired speed under the external load (inertia of the end-effector can also be counted as an external load in this approach) with a specified norm acting from the "worst" direction. Thus, the extremal value of the power output can be calculated for a driving mechanism. There may be several work-arounds for improving this approach, but this is also beyond the scope of this paper.

3. Screw Theory Approach

Now, let us consider the screw theory approach for the same problem. It is well known that the following equation holds for any leg of parallel mechanism:

$$\sum_{j=1}^{N_i} \mathbf{t}_{i,j} \cdot \dot{q}_{i,j} = \mathbf{\Omega}, \tag{5}$$

where $\mathbf{t}_{i,j}$ is the unit twist of the jth pair in the ith leg, $\dot{q}_{i,j}$ is the corresponding velocity in this pair, $\mathbf{\Omega}$ is the twist of the end-effector, and N_i is the total number of kinematic pairs in the leg. Since we require exactly six scalar components to represent a screw,[23] $\mathbf{\Omega} \neq \dot{\mathbf{x}}$ if $n < 6$.

Using the reciprocal screw approach[24] and considering $\dot{q}_{i,1} = \dot{\theta}_i$, we obtain the following for each leg:

$$\dot{\theta}_i \cdot \mathbf{t}_{i,1} \circ \mathbf{w}_i = \mathbf{\Omega} \circ \mathbf{w}_i. \tag{6}$$

Here "$\circ$" denotes the reciprocal product of a twist and a wrench, and $\mathbf{w}_i$ is the wrench reciprocal for all unit twists from (5) except $\mathbf{t}_{i,1}$:

$$\mathbf{w}_i \circ \mathbf{t}_{i,j} = 0 \quad \forall j = 2, \ldots, N_i. \tag{7}$$

Let us denote the twist of the end-effector that maximizes $|\dot{\theta}_i|$ as $\mathbf{\Omega}_i^{\max}$. From Eq. (6), one can clearly see that $|\dot{\theta}_i| = |\dot{\theta}_i|^{\max}$ for a given constant $\|\mathbf{\Omega}\|$ if $\mathbf{\Omega} = \mathbf{\Omega}_i^{\max}$ is proportional to $\mathbf{w}_i$ in the following manner:

$$\mathbf{\Omega}_i^{\max} \propto \begin{bmatrix} \mathbf{0}_{3\times 3} & \mathbf{I}_3 \\ \mathbf{I}_3 & \mathbf{0}_{3\times 3} \end{bmatrix} \cdot \mathbf{w}_i.$$

For a 6-DOF mechanism, $\mathbf{w}_i$ is defined uniquely up to a non-zero multiplier, as the twist space of passive joints for each leg will have the dimensionality of five (as per the assumptions from the first section). Therefore, the dimensionality of the orthogonal complement space will be equal to one.

For any mechanism with less than six DOFs, this wrench should also not be a part of the constraint wrench space $\mathbf{W}_i^c$ of the ith leg:

$$\mathbf{w}_i \notin \mathbf{W}_i^c = \left\{ \mathbf{w}_i^c \;\middle|\; \mathbf{w}_i^c \circ \mathbf{t}_{i,j} = 0 \quad \forall j = 1, \ldots, N_i \right\}.$$

In actuality, we are interested in finding the twist $\mathbf{\Omega}_i^{\max}$ and not the wrench $\mathbf{w}_i$ itself, and since this twist should not be constrained by any leg, we can replace this condition with a stronger one:

$$\mathbf{w}_i \perp \mathbf{W}_i^c. \tag{8}$$

Thus, conditions (7) and (8) will define $\mathbf{w}_i$ and, consequently, $\mathbf{\Omega}_i^{\max}$ uniquely up to a non-zero multiplier. These conditions, however, do not guarantee that this twist will be feasible for the mechanism (each leg can be represented as a linear combination of the joint twists of this leg). To ensure this, we must consider an orthogonal projection of the $\mathbf{\Omega}_i^{\max}$ onto the freedom space $\mathbf{\Phi}$ of the mechanism:

$$\mathbf{\Omega}_{\mathbf{\Phi} i}^{\max} = \operatorname{proj}_{\mathbf{\Phi}}\left(\mathbf{\Omega}_i^{\max}\right) = \sum_{p=1}^{n} \frac{\left\langle \mathbf{\Omega}_i^{\max}, \boldsymbol{\phi}_p \right\rangle}{\left\langle \boldsymbol{\phi}_p, \boldsymbol{\phi}_p \right\rangle} \cdot \boldsymbol{\phi}_p$$

and calculate $|\dot{\theta}_i|$ for $\mathbf{\Omega} = \mathbf{\Omega}_{\mathbf{\Phi} i}^{\max}$. Here, $\boldsymbol{\phi}_1, \boldsymbol{\phi}_2, \ldots, \boldsymbol{\phi}_n$ is the orthogonal basis of $\mathbf{\Phi}$. The freedom space contains all feasible end-effector twists*******:

$$\mathbf{\Phi} = \bigcap_{i=1}^{n} \operatorname{Span}(\mathbf{t}_{i,1}, \mathbf{t}_{i,2} \ldots, \mathbf{t}_{i,N_i}).$$

The orthogonal projection here is, in fact, the twist $\mathbf{\Omega}_i^{\max}$ that has corresponding Plücker coordinates for the infeasible motions of the end-effector set to zero.

Finally, the maximum possible magnitude of the actuated joint velocity in the i-th leg can be calculated using the following equation:

$$|\dot{\theta}_i|^{\max} = |\dot{\theta}_i|_{\omega}^{\max} + |\dot{\theta}_i|_{v}^{\max} = \left|\frac{\mathbf{\Omega}_{\mathbf{\Phi}i(\boldsymbol{\omega})}^{\max} \circ \mathbf{w}_i}{\mathbf{t}_{i,1} \circ \mathbf{w}_i}\right| + \left|\frac{\mathbf{\Omega}_{\mathbf{\Phi}i(\mathbf{v})}^{\max} \circ \mathbf{w}_i}{\mathbf{t}_{i,1} \circ \mathbf{w}_i}\right|.$$

where $\mathbf{\Omega}_{\mathbf{\Phi}i(\boldsymbol{\omega})}^{\max}$ and $\mathbf{\Omega}_{\mathbf{\Phi}i(\mathbf{v})}^{\max}$ are obtained by setting all linear or angular components of $\mathbf{\Omega}_{\mathbf{\Phi}i}^{\max}$ to zero respectively. These twists are normalized separately.

Now, let us assume that all the actuated joints are locked. The wrench system of the mechanism will then consist of n wrenches $\mathbf{w}_i$. We can also define the constraint space of the mechanism as follows:

$$\mathbf{W}^c = \bigcup_{i=1}^{n} \mathbf{W}_i^c.$$

The constraint space can be represented by $6-n$ linearly independent constraint wrenches $\mathbf{w}^c$. If the constraint spaces of different legs intersect each other, then wrenches $\mathbf{w}^c$ can actually be chosen arbitrarily within $\mathbf{W}^c$. Assuming that the mechanism is in a state of equilibrium, its static analysis can be executed using the following equation:

$$\sum_{i=1}^{n} r_i \cdot \mathbf{w}_i + \sum_{k=1}^{6-n} r_i^c \cdot \mathbf{w}_k^c = \mathbf{L}. \tag{9}$$

where $\mathbf{L}$ is a six-component wrench of external load and r_i, r_i^c are generalized reactions that define the actual magnitude of corresponding wrenches. Note that $\mathbf{L} \neq \mathbf{F}$ if $n < 6$.

Using the same approach, we can reduce (9) to

$$r_i \cdot \mathbf{w}_i \circ \boldsymbol{\tau}_i = \mathbf{L} \circ \boldsymbol{\tau}_i,$$

where $\boldsymbol{\tau}_i$ is defined using the following conditions:

$$\boldsymbol{\tau}_i \circ \mathbf{w}_k^c = 0 \quad \forall \mathbf{w}_k^c \in \mathbf{W}^c; \qquad \boldsymbol{\tau}_i \circ \mathbf{w}_i \neq 0; \qquad \boldsymbol{\tau}_p \circ \mathbf{w}_{pi} = 0 \quad \forall p \neq i \quad (p = 1..n).$$

Unlike $\mathbf{w}^i$, this twist will always be defined uniquely up to a non-zero multiplier even if $n < 6$. Thus, we can maximize $|r_i|$ by assuming the components of $\mathbf{L} = \mathbf{L}_i^{\max}$ to be proportional to the components of $\boldsymbol{\tau}_i$:

$$\mathbf{L}_i^{\max} \propto \begin{bmatrix} \mathbf{0}_{3\times 3} & \mathbf{I}_3 \\ \mathbf{I}_3 & \mathbf{0}_{3\times 3} \end{bmatrix} \cdot \boldsymbol{\tau}_i.$$

The maximum possible generalized reaction in the i-th leg can be calculated as follows:

$$|r_i|^{\max} = |r_i|_{\omega}^{\max} + |r_i|_{v}^{\max} = \left|\frac{\mathbf{L}_{i(\boldsymbol{\omega})}^{\max} \circ \boldsymbol{\tau}_i}{\mathbf{w}_i \circ \boldsymbol{\tau}_i}\right| + \left|\frac{\mathbf{L}_{i(\mathbf{v})}^{\max} \circ \boldsymbol{\tau}_i}{\mathbf{w}_i \circ \boldsymbol{\tau}_i}\right|.$$

where $\mathbf{L}_{i(\boldsymbol{\omega})}^{\max}$ and $\mathbf{L}_{i(\mathbf{v})}^{\max}$ are obtained by setting all linear (forces) or all angular (torques) components of $\mathbf{L}_i^{\max}$ respectively to zero, and these should be normalized independently.

It is important to distinguish between the generalized reaction r_i and the actuation effort e_i. The first is simply a multiplier that, in fact, should be considered together with the corresponding wrench $\mathbf{w}^i$ in order to represent the component of the external load that acts on this particular leg. The actuation effort can be calculated from $r_i \cdot \mathbf{w}^i$ by changing the reference point for the Plücker coordinates of $r_i \cdot \mathbf{w}^i$ from the point on the end-effector to the point that defines the position of the actuated joint. Then, the actuation effort will be just the component of this wrench that corresponds to the actuated degree of freedom of the i-th active joint.

It is also extremely important to note that the notions of reciprocal and perpendicular screws used previously are practically the same; in the sense that they describe the elements of the orthogonal complement subspace in a six-dimensional screw (vector) space. However, the notions of the orthogonal complement and orthogonal projection are not well-defined for the twist or wrench spaces.

https://doi.org/10.1017/S026357471800125X Published online by Cambridge University Press

On the other hand, these notions and the orthogonal projection operator are used only for intermediate calculations. In the end, the numerical results are physically meaningful. This has been demonstrated in the case-study section by comparing the results obtained from the Jacobian analysis and Screw theory-based approaches with the simulation results.

The other problem is that the screw components depend on the choice of the reference frame or, more precisely, on the choice of the reference point.[23] Since we are interested in the movement of the end-effector and the load applied to it, it is clear that the reference point for all screws should be the point on the end-effector—the so-called "operating point"[1] (see the first case study section).

Overall, the Screw theory-based approach is computationally more demanding and less stable (at least in our case study calculations) than the Jacobian analysis approach. However, it allows one to also perform the velocity analysis for passive joints. Additionally, for the static analysis, it deals not only with the actuation efforts but also with the load on the leg as a whole, allowing the calculation of stresses and reactions if required. Also, it can possibly allow one to consider the so-called constraint singularities[25] through the analysis of the generalized reactions corresponding to the constraint wrenches. However, this is beyond the scope of this paper.

4. Closeness to Singularity

It is a well-known fact that the actuated joint velocities increase when a mechanism approaches the serial (Type 1 as described in ref. [17]) singularity, and the actuation efforts are larger near the parallel (Type 2 as described in ref. [17]) singularity. Thus, these two parameters are a natural measure of the closeness to these types of singularities.

Perhaps the most extensive study of the closeness to singularities for parallel mechanisms can be found in Voglewede's articles on the subject.[20,21] In this work, the task of calculating a measure of the closeness to singularity (in the velocity domain) is formulated as the constraint optimization problem:

$$M = \begin{cases} \min \quad \dot{\boldsymbol{\theta}}^T \mathbf{S} \dot{\boldsymbol{\theta}} \\ \text{subject to} \\ \dot{\boldsymbol{\theta}} - \mathbf{J}^{\text{inv}} \dot{\mathbf{x}} = 0 \\ \dot{\mathbf{x}}^T \mathbf{T} \dot{\mathbf{x}} - 1 = 0 \end{cases}$$

which is then transformed into a generalized eigenvalue problem. The solution to the latter is well-known. The formulation for the force domain is similar.

The choice of scaling matrices $\mathbf{S}$ and $\mathbf{T}$ defines the physical meaning of the measure M. Voglewede, in his second paper, provides nine different combinations for these matrices in each domain and notes that, though the list he provides is not exhaustive, almost all possible measures can be formulated in this manner.

The usage of the actuated joint velocities as the measure of closeness to the serial singularity can also be written using Voglewede's notation:

$$M_\theta = \max_{i=1,\dots,N_a} \left(\sqrt{|\dot{\theta}_i|_\omega^{\max}} + \sqrt{|\dot{\theta}_i|_v^{\max}} \right),$$

where, for each i,

$$|\dot{\theta}_i|_\omega^{\max} = \begin{cases} \max \quad \theta_i^2 \\ \text{subject to} \\ \dot{\boldsymbol{\theta}} - \mathbf{J}_\omega^{\text{inv}} \boldsymbol{\omega} = 0 \\ \|\boldsymbol{\omega}\|^2 = c_\omega \end{cases}, \qquad |\dot{\theta}_i|_v^{\max} = \begin{cases} \max \quad \theta_i^2 \\ \text{subject to} \\ \dot{\boldsymbol{\theta}} - \mathbf{J}_v^{\text{inv}} \mathbf{v} = 0 \\ \|\mathbf{v}\|^2 = c_v \end{cases}.$$

Matrices $\mathbf{J}_\omega^{\text{inv}}$ and $\mathbf{J}_v^{\text{inv}}$ consist only of columns of $\mathbf{J}^{\text{inv}}$ that correspond to the $\boldsymbol{\omega}$ and $\mathbf{v}$, while c_ω and c_v are some given constants that are equal to the square of the desired values of angular and linear velocities of the end-effector, respectively.

These formulae imply that, for each leg, the scaling matrix $\mathbf{S}$ is a diagonal matrix consisting only of zeroes except its i, i-th component, which is equal to one. It is also implied that $\mathbf{T}$ is an identity matrix. However, the significant part is that it is defined for the angular and linear parts of $\dot{\mathbf{x}}$ separately (also note that here we normalize vectors $\boldsymbol{\omega}$ and $\mathbf{v}$, not $\dot{\mathbf{x}}$):

$$\mathbf{T}_\omega = \mathbf{I}_{\dim(\boldsymbol{\omega})}, \qquad \mathbf{T}_v = \mathbf{I}_{\dim(\mathbf{v})}.$$

Similarly, for parallel singularities, we can write the following:

$$M_e = \max_{i=1,\dots,N_a} \left(\sqrt{|e_i|_\omega^{\max}} + \sqrt{|e_i|_v^{\max}} \right),$$

where, for each i,

$$|e_i|_\omega^{\max} = \begin{cases} \max \quad e_i^2 \\ \text{subject to} \\ \mathbf{e} + \mathbf{J}_f^T \mathbf{f} = 0 \\ \|f\|^2 = c_f \end{cases} \qquad |e_i|_\omega^{\max} = \begin{cases} \max \quad e_i^2 \\ \text{subject to} \\ \mathbf{e} + \mathbf{J}_m^T \mathbf{m} = 0 \\ \|m\|^2 = c_m \end{cases}$$

Here, matrices $\mathbf{J}_f^T$ and $\mathbf{J}_m^T$ consist only of columns of $\mathbf{J}^T$ that correspond to $\mathbf{f}$ and $\mathbf{m}$ respectively, and c_ω and c_v are the constants given.

There are, however, some differences between this approach and the work of Voglewede. First of all, the discussed measures do not obey the rules established in the referenced papers, as they increase when the mechanism is close to its singularity. However, one can simply consider the reciprocal values of these measures.

Another difference is in the weighting matrices $\mathbf{S}$ and $\mathbf{T}$. Here, we use two separate matrices $\mathbf{T}$ for different types of DOFs, practically separating angular and linear components in order to avoid the units' inconsistency. In Voglewede's paper matrix, $\mathbf{S}$ is assumed to be invertible, while this is not the case in the Jacobian matrix. However, if the correct Jacobian (direct or inverse) matrix is chosen, there is no need to consider the inverse of $\mathbf{S}$ or $\mathbf{T}$ matrices.

Thus, one can see that the discussed approach can be technically treated as a special case within Volglewede's framework (as virtually any closeness to singularity measure can). However, it still has some differences that allow one to avoid the usage of non-kinematic properties while still maintaining the practicality and applicability of the presented measures.

5. Case Study: 3-RRRRR Translational Parallel Mechanism

To demonstrate the discussed approach, we will use a 3-DOF translational parallel mechanism. The mechanism and the unit twists of its legs are shown in Fig. 1.

The workspace of this mechanism is covered by a grid of certain steps. Then, we calculate the inverse Jacobian matrix $\mathbf{J}^{\text{inv}}$ for each node by taking the partial derivatives of the mechanism's constraint equations (more details regarding the singularity analysis of this mechanism are furnished in ref. [26]). Thereafter, we calculate the transpose Jacobian matrix, which is equal to $(\mathbf{J}^{\text{inv}})^{-T}$, after which we calculate $|\dot{\theta}_i|^{\max}$ and $|e_i|^{\max}$ using Eqs. (1) and (2). We can use these equations instead of (3) and (4) because the mechanism only has translational degrees of freedom.

For the Screw theory-based analysis, the following algorithm is executed in every node:

1. We calculate the Plücker coordinates of each unit twist $\mathbf{t}_{i,j}$ with the end-effector's operating point (F on Fig. 1) as the reference.
2. Using the Plücker coordinates of joint twists, a 5×6 matrix $\mathbf{T}_i$ is formed for each leg:

$$\mathbf{T}_i = \begin{pmatrix} \mathbf{t}_{i,1}^T \\ \vdots \\ \mathbf{t}_{i,5}^T \end{pmatrix}.$$

3. A kernel of each matrix is found to provide us with a twist $\mathbf{t}_{\mathbf{w}i}^c$ that is proportional to the constraint wrench $\mathbf{w}_i^c$.

https://doi.org/10.1017/S026357471800125X Published online by Cambridge University Press

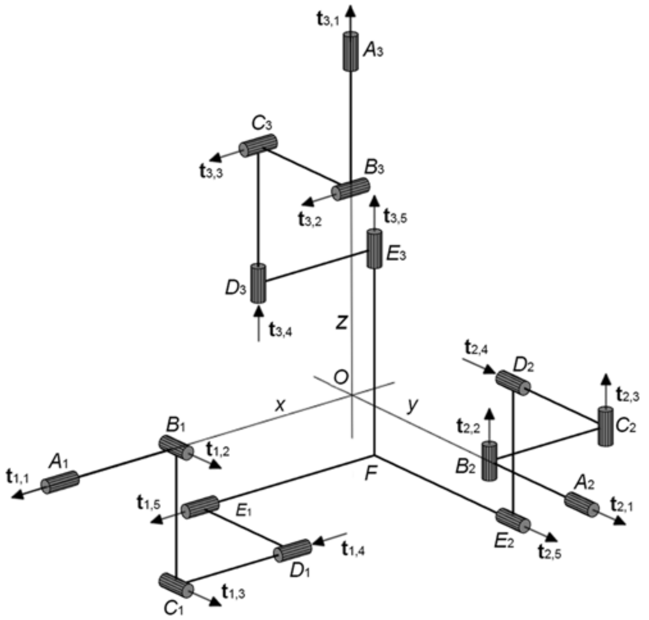

Fig. 1. 3-DOF Translational Parallel Manipulator and corresponding unit twists.

4. The Plücker coordinates of the actuated joint twist $\mathbf{t}_{i,1}$ (first row of $\mathbf{T}_i$) are replaced with Plücker coordinates of $\mathbf{t}^c_{\mathbf{w}i}$, and the kernel of this newly formed matrix is calculated (for each leg). This essentially gives us the components of twist $\mathbf{\Omega}_i^{\max}$.
5. Since we deal with a translational mechanism, all rotational components of $\mathbf{\Omega}_i^{\max}$ are then replaced by zeroes, providing a twist $\mathbf{\Omega}_{\mathbf{\Phi}i}^{\max}$. At this point, we can normalize this twist to a certain given norm and calculate the maximized values of angular velocities in the actuated joints $|\dot{\theta}_i|^{\max}$ for each leg.
6. The Plücker coordinates of $\mathbf{t}^c_{\mathbf{w}i}$ and $\mathbf{\Omega}_i^{\max}$ for all three legs are rearranged to form a 6×6 matrix $\mathbf{W}$ so that each row of this matrix consists of components of $\mathbf{w}_i^c$ or $\mathbf{w}_i$:

$$\mathbf{W} = \begin{pmatrix} (\mathbf{w}_1^c)^T \\ \mathbf{w}_1^T \\ \vdots \\ (\mathbf{w}_3^c)^T \\ \mathbf{w}_3^T \end{pmatrix}.$$

7. For each leg, the row corresponding to $\mathbf{w}_i$ of this leg is excluded, and the kernel of the remaining 5×6 matrix is then calculated. Thus, we obtain external load wrenches $\mathbf{L} = \mathbf{L}_i^{\max}$ corresponding to $|r_i|^{\max}$ for each leg.
8. $\mathbf{L}_i^{\max}$ is normalized to a given norm and the value of $|r_i|^{\max}$ is calculated. Then, for each leg, an actuation effort $|e_i|^{\max}$ is found by moving the Plücker coordinates reference point of $r_i \cdot \mathbf{w}_i$ from point F to point A_i.

In this example, we assume that the lengths of the links are (in centimetres): $l_1 = A_iB_i = 20$, $l_2 = B_iC_i = 20$, $l_3 = C_iD_i = 20$, $l_4 = D_iE_i = 20$, $l_5 = E_iF = 30$, $l_A = OA_i = 50$. We also assume that the discretization step is 0.2 cm. In order to provide a clear visualization using 2-D plots, we also fix the Cartesian coordinate z of the end-effector on a certain constant value (in this case -18 cm).

In Fig. 2, a slice of the workspace is presented. In each point, the value of rotational speed ν in the actuated joints (in revolutions per minute) is calculated for each leg using the discussed approach and assuming that the end-effector velocity is 100 cm/s. Thereafter, the largest of the three (one for each leg) values is associated with its corresponding point. All points are divided in four sets depending on whether the magnitude of their rotational speed exceeds a certain threshold value. The dashed black line represents the points when a serial singularity occurs, and the white area is not a part of

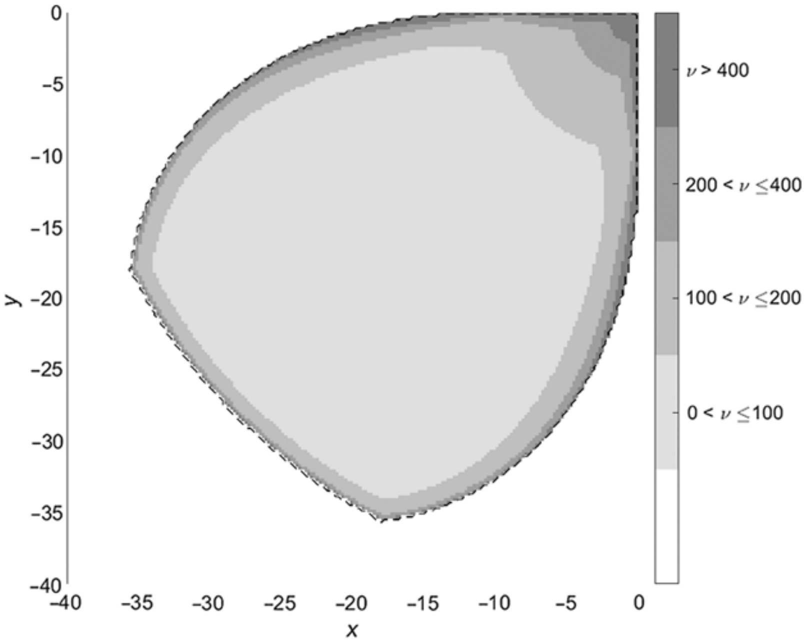

Fig. 2. Slice of the mechanism workspace and corresponding maximized rotational speed in actuated joints.

the workspace. One can clearly see that the rotational speed in the actuated joints increases near the singularity.

If, for instance, the driving mechanism of any actuated joint is not capable of producing more than 100 rpm, the "effective" workspace, that is, the workspace when a desirable end-effector speed of 100 cm/s can be achieved, will shrink to the light-grey area in Fig. 2.

In practice, the parallel singularity usually has more impact on the mechanism's performance than the serial singularity. The location of the parallel singularity points depends on the mechanism configuration, which corresponds to a certain set of input angles[26] defined by the working mode.

There are two "optimal" configurations in which parallel singularities have less of a possible influence on the workspace volume (due to the mechanism geometry): $(\theta_{1,1}, \theta_{2,1}, \theta_{3,1})$ and $(\theta_{1,2}, \theta_{2,2}, \theta_{3,2})$. All the calculations we performed earlier in this paper correspond to the set of angles $(\theta_{1,2}, \theta_{2,2}, \theta_{3,2})$.

Let us consider the same slice of the mechanism workspace again. Now, each point will correspond to the maximum absolute value of actuation effort (in N·cm) calculated using the discussed approach for an external force of 10 N acting on the end-effector. The result for the optimal configuration $(\theta_{1,2}, \theta_{2,2}, \theta_{3,2})$ is shown in Fig. 3, and that for the non-optimal configuration $(\theta_{1,2}, \theta_{2,1}, \theta_{3,1})$ is shown in Fig. 4. Again, all the points are separated into four sets by certain threshold values, and the dashed black line marks the location of points corresponding to a parallel singularity.

All calculations are done on a laptop (Core-i7 CPU and 16 GB RAM) in MATLAB using its built-in functions for system solving, matrix inversion, etc. During the iteration process, 132,651 points within the mechanism's workspace have been analyzed. For each point, we have calculated the relative deviation between the results obtained using the Jacobian and Screw theory-based analyses:

$$\Delta_{\dot\theta}^{\max} = \left| \frac{|\dot\theta|_{\mathrm{Jac}} - |\dot\theta|_{\mathrm{Scr}}}{|\dot\theta|_{\mathrm{Jac}}} \right| = 7.9375 \cdot 10^{-15}, \quad \Delta_{e}^{\max} = \left| \frac{|e|_{\mathrm{Jac}} - |e|_{\mathrm{Scr}}}{|e|_{\mathrm{Jac}}} \right| = 2.1150 \cdot 10^{-14}.$$

Here, $\Delta_e^{\max}$ and $\Delta_{\dot\theta}^{\max}$ are the maximum values of deviations between the magnitudes of $|e| = |e|^{\max}$ and $|\dot\theta| = |\dot\theta|^{\max}$, respectively; indices $_{\mathrm{Jac}}$ and $_{\mathrm{Scr}}$ denote the method of obtaining the value based on the Jacobian analysis or on the Screw theory, respectively.

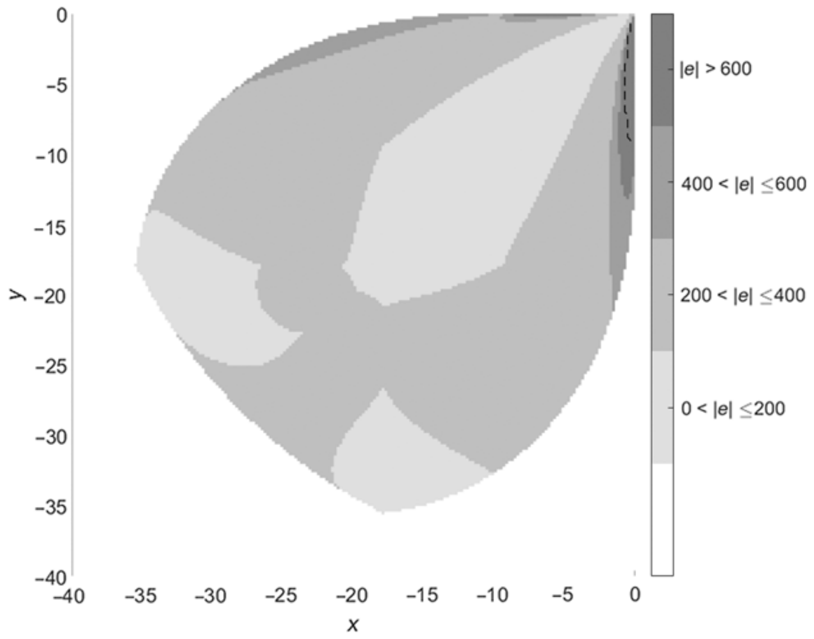

Fig. 3. Slice of the mechanism workspace and corresponding maximized actuation efforts in optimal configuration.

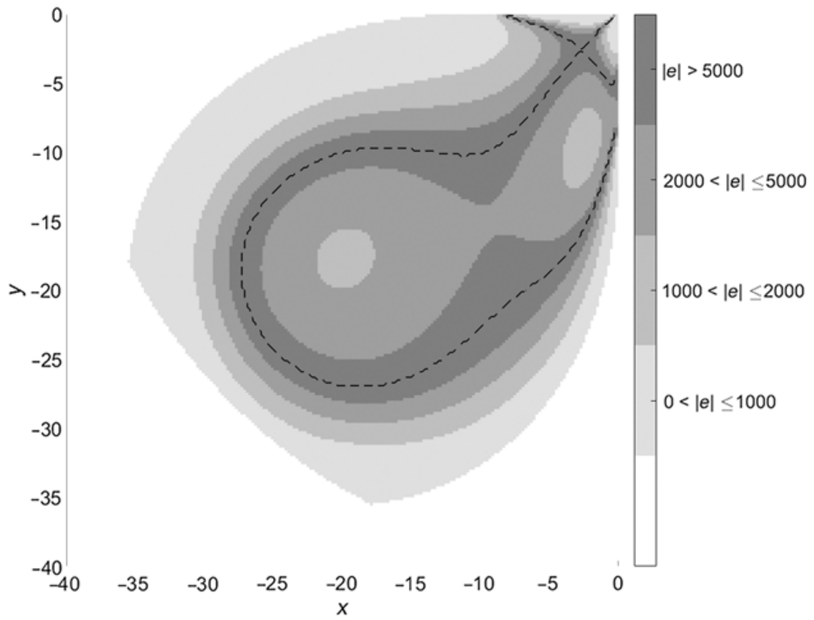

Fig. 4. Slice of the mechanism workspace and corresponding maximized actuation efforts in non-optimal configuration.

We have also calculated the deviation between the Jacobian analysis approach and the method described by Voglewede (index $_{\text{Eig}}$) for each point:

$$\Delta_{\dot{\theta}}^{\max} = \left| \frac{|\dot{\theta}|_{\text{Jac}} - |\dot{\theta}|_{\text{Eig}}}{|\dot{\theta}|_{\text{Jac}}} \right| = 8.7235 \cdot 10^{-16}, \quad \Delta_{e}^{\max} = \left| \frac{|e|_{\text{Jac}} - |e|_{\text{Eig}}}{|e|_{\text{Jac}}} \right| = 8.4908 \cdot 10^{-16}.$$

https://doi.org/10.1017/S026357471800125X Published online by Cambridge University Press

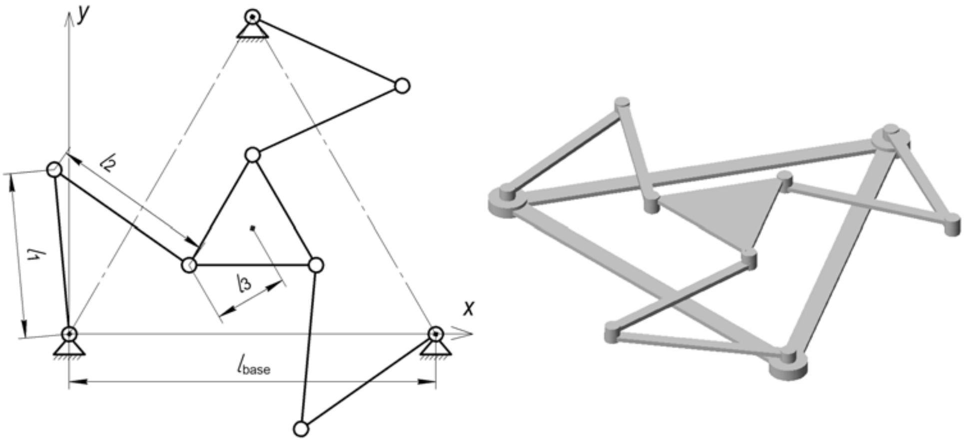

Fig. 5. Scheme of 3-RRR planar mechanism and its model.

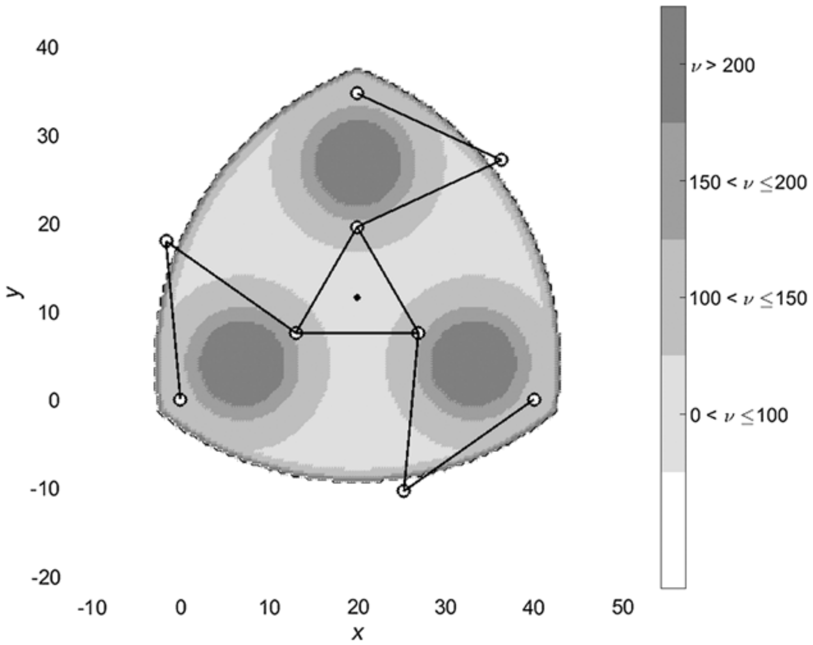

Fig. 6. Constant orientation workspace and corresponding maximized rotational speed in actuated joints.

In each point, the time required to perform the calculation (excluding the time spent on inverse kinematics problem) was measured (in seconds) as follows:

Value	Jacobian analysis	Screw theory	Eigenvalue problem
$\lvert\dot{\theta}\rvert^{\max}$	$3.56 \cdot 10^{-5}$	$3.70 \cdot 10^{-4}$	$6.44 \cdot 10^{-5}$
$\lvert e\rvert^{\max}$	$3.31 \cdot 10^{-5}$	$3.16 \cdot 10^{-4}$	$4.96 \cdot 10^{-5}$

The actuation effort calculation is faster because it uses the results that were already obtained during the joint velocity calculations.

Thus, in conclusion, we can see that the discussed approach does indeed function as intended. The deviation between the results obtained using the Jacobian analysis and the Screw theory-based calculation method is negligible. Comparing this approach and the Voglewede's method, one can

https://doi.org/10.1017/S026357471800125X Published online by Cambridge University Press

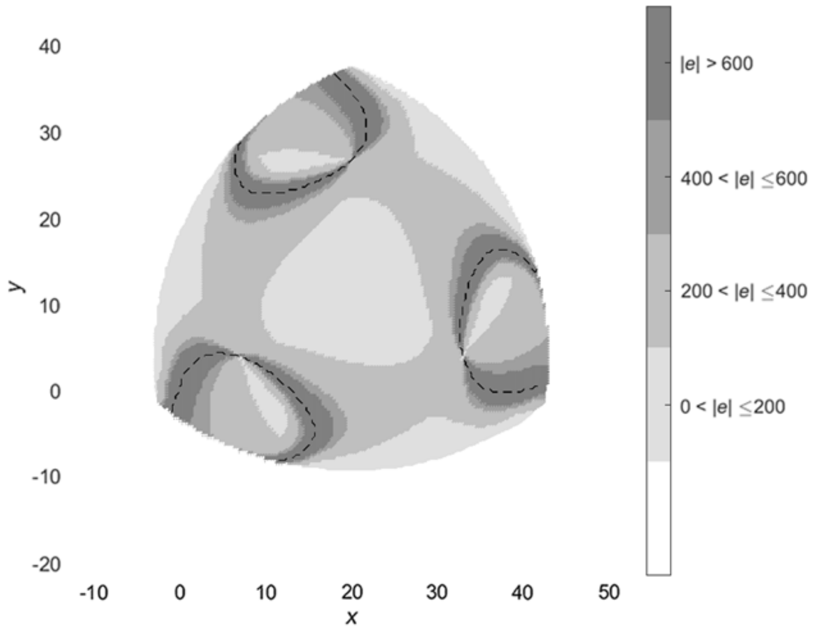

Fig. 7. Constant orientation workspace and corresponding maximized actuation efforts (first configuration).

also see that the numerical results are the same for the joint velocity analysis. It can also be seen that, at least in MATLAB, the Jacobian analysis method is about 10 times faster for computing than the Screw-based one and about twice as fast as compared to Voglewede's method.

6. Case Study: 3-RRR Planar Parallel Mechanism

Let us now consider a classical 3-RRR planar parallel mechanism (Fig. 5) to demonstrate that the angular and linear components of vectors can be analyzed separately.

The dimensions of this mechanism are $l_{\text{base}} = 40$ cm, $l_1 = 18$ cm, $l_2 = 18$ cm, and $l_3 = 8$ cm. Essentially, using the same algorithm as earlier, the workspace of this mechanism was analyzed. The result of a generalized velocity analysis for a constant-orientation workspace and a scaled schematic image of the mechanism itself are illustrated in Fig. 6. The end-effector velocity is 100 cm/s, discretization step is 0.2 cm, and the unit of rotation speed in actuated joints is rpm.

One can clearly see that the rotation speed in actuated joints is higher when the end-effector is close to the serial singularity curve, which is the workspace boundary (dashed line). However, there are three circular areas within the workspace in which the rotation speed is also increased. This occurs due to the fact that the centre points of these circles are "Type 3"[17] singular, which was demonstrated in ref. [27].

The results of an actuation effort analysis are presented in Figs. 7 and 8 for two different mechanism configurations (working modes). The external force is 10 N and actuation effort units are N·cm.

Again, the actuation efforts clearly increase as the end-effector approaches a parallel singularity. However, one can see that the "Type 3" singular points, which were discussed before, can be approached from certain directions without significantly altering the actuation effort's magnitude. A closer look with an iteration step 0.005 cm of one of these points (for a second working mode) is shown in Fig. 9.

We have simply ignored the angular velocity and torque component of the end-effector twist and the external load wrench, respectively.

Now, we use a Simulink model to compare the actuation efforts produced by an external force applied to the moving plate. We simulate a trajectory that is a "rose" curve with three loops (Fig. 10). The simulation time is 15 s, and the coordinates of this curve's points are calculated with a 0.01 s step.

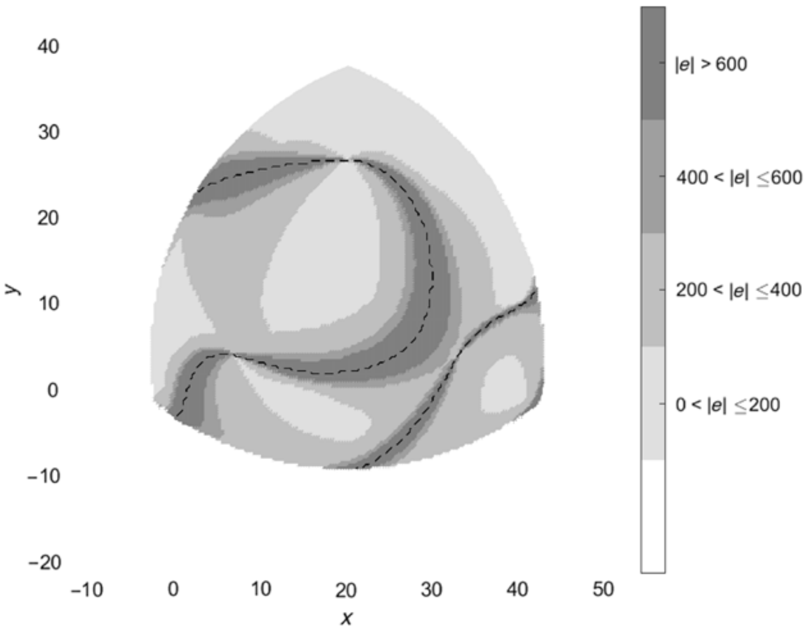

Fig. 8. Constant orientation workspace and corresponding maximized actuation efforts (second configuration).

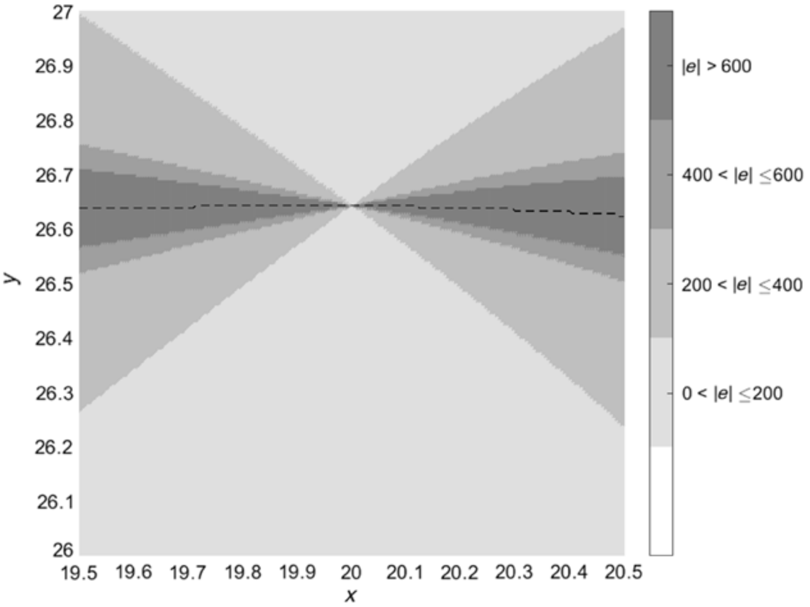

Fig. 9. Distribution of maximized actuation efforts near a "Type" 3 singular point (second configuration).

In each point, a force of 10 N is applied to the moving plate from three different directions: parallel to x-axis, parallel to y-axis, and the third direction is calculated using the aforementioned approach.

The simulation results indicate that this is indeed true. In Fig. 11, the absolute value of an actuation effort in the first leg $|e_1|$ is shown as an example. Curve "1" corresponds to a force direction obtained using the discussed approach, while the curves "2" and "3" correspond to the forces parallel to x- and y-axis, respectively. Clearly, one can see that curve "1" corresponds to the maximum possible actuation effort for any given moment of simulation.

https://doi.org/10.1017/S026357471800125X Published online by Cambridge University Press

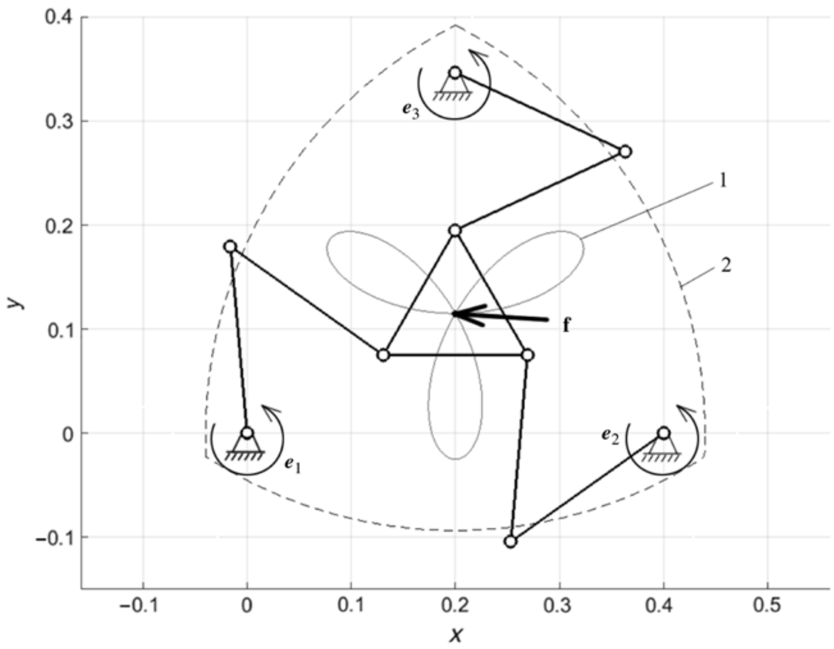

Fig. 10. Simulation scheme. 1: Moving plate trajectory; 2: Workspace boundary.

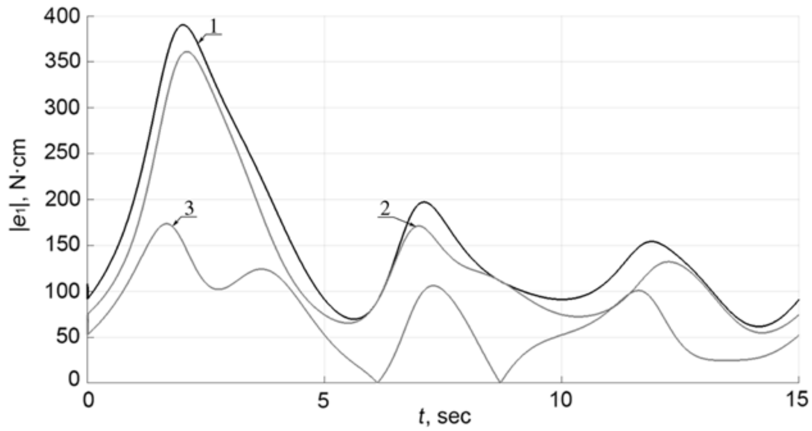

Fig. 11. Actuation effort in the first leg for different directions of external force.

7. Conclusion

The Jacobian analysis-based calculation method discussed in this paper allows one to easily calculate the maximum possible absolute value of the actuated joint velocity or the actuation efforts in each leg of a parallel mechanism. The Screw theory-based alternative method, which allows one to also consider passive joints velocities or generalized reactions in the leg, has also been presented. It has also been shown that both methods yield the same results during the calculation. However, at least in this particular study, the second method requires more computational time and should also be used with certain care, as it partially depends on the reference frame choice.

The key aspect of both the methods is that the angular and linear components of end-effector velocity and external load vectors (screws) are treated separately.

The possible usage of the mentioned values as the measure of closeness to serial or parallel singularity has been discussed. It has also been demonstrated that, although the approach can be treated as the special case of the state-of-the-art framework (namely, the one developed by Voglewede), it has its strengths and weaknesses. One of its possible advantages is that it relies only on kinematic or static properties of the mechanism. The other one is that it uses highly natural measures that depend on the mechanism's drives, performance, and characteristics, which can be taken into account relatively easily. The comparative study of the discussed approach and the Voglewede's computational method in a case study of the 3-DOF translational parallel mechanism indicates that the numerical results are the same for the velocity and actuation effort analysis. The case study of a 3-DOF planar parallel mechanism has also been presented to demonstrate the possibility of the separation of different DOF types during the calculation.

The discussed methods yielded expected results in both case studies. This fact makes it possible to conclude that the discussed approach can be used for any parallel mechanism that corresponds to the assumptions presented in the introduction section of this paper.

Acknowledgments
This work is carried out in the basic part of the state task for performing scientific research No. 9.5309.2017/8.9 and RFBR grant 15-51-06002 MNTIa "Development of Topologies of Robots with Parallel Structure and New Methods of Analyzing Their Singularities."

References
1. J.-P. Merlet, *Parallel Robots*, 2nd edition (Springer, Dordrecht, Netherlands, 2006), 402 pp.
2. C. M. Gosselin and L. Schreiber, "Kinematically redundant spatial parallel mechanisms for singularity avoidance and large orientational workspace," *IEEE Trans. Robot.* **32**(2), 286–300 (2016).
3. R. Di Gregorio, "Kinematics analysis and singularities of novel decoupled parallel manipulators with simplified architecture," *Robotica* **35**(4), 961–979 (2017).
4. St-Onge B. Mayer and C. M. Gosselin, "Singularity analysis and representation of the General Gough–Stewart platform," *Int. J. Robot. Res.* **19**(3), 271–288 (2000).
5. J.-P. Merlet, "Singular configurations of parallel manipulators and Grassmann geometry," *Int. J. Robot. Res.* **8**(5), 45–56 (1989).
6. D. Chablat, Ph. Wenger and J. Angeles, "The Isoconditioning Loci of a Class of Closed-Chain Manipulators," *Proceedings of the IEEE International Conference on Robotics and Automation*, Anchorage, AK, USA (2010) pp. 1970–1976.
7. J. F. O'Brien and J. T. Wen, "Kinematic Control of Parallel Robots in the Presence of Unstable Singularities," *Proceedings of the IEEE International Conference on Robotics and Automation*, Seoul, South Korea (2001) pp. 3154–3159.
8. S. Sen, B. Dasgupta and A. K. Mallik, "Variational approach for singularity-path planning of parallel manipulators," *Mech. Mach. Theory* **38**(11), 1165–1183 (2003).
9. S. Bhattacharya, H. Hatwal and A. Ghosh, "Comparison of an exact and an approximate method of singularity avoidance in platform type parallel manipulators," *Mech. Mach. Theory* **33**(7), 965–974 (1998).
10. C. M. Gosselin and J. Angeles, "A global performance index for the kinematic optimization of robotic manipulators," *J. Mech. Des.* **113**(3), 220–226 (1991).
11. J.-P. Merlet, "Jacobian, manipulability, condition number, and accuracy of parallel robots," *J. Mech. Des.* **128**(1), 199–205 (2006).
12. C. Chen and J. Angeles, "A Generalized Transmission Index for Spatial Linkages," *Proceedings of the ASME 2005 IDETC/CIE Conference*, Long Beach, CA, USA (2005) pp. 749–756.
13. S. Balli and S. Chand, "Transmission angle in mechanisms," *Mech. Mach. Theory* **37**(2), 175–195 (2002).
14. O. Alba-Gomez, P. Wenger and A. Pamanes, "Consistent Kinetostatic Indices for Planar 3-DOF Parallel Manipulators, Application to the Optimal Kinematic Inversion," *Proceedings of the ASME 2005 IDETC/CIE Conference*, Long Beach, CA, USA (2005) pp. 765–774.
15. S. Briot, A. Pashkevich and D. Chablat, "Optimal Technology-oriented Design of Parallel Robots for High-speed Machining Applications," *Proceedings of the 2010 IEEE International Conference on Robotics and Automation (ICRA 2010)*, Anchorage, AK, USA (2010) pp. 1155–1161.
16. G. Sutherland and B. Roth, "A transmission index for spatial mechanisms," *J. Manuf. Sci. Eng.* **95**(2), 589–597 (1973).
17. C. M. Gosselin and J. Angeles, "Singularity analysis of closed-loop kinematic chains," *IEEE Trans. Rob. Autom.* **6**(3), 281–290 (1990).
18. D. Zlatanov, R. G. Fenton and B. Benhabib, "A unifying framework for classification and interpretation of mechanism singularities," *J. Mech. Design* **117**(4), 566–572 (1995).
19. J. Hubert and J.-P. Merlet, "Static of parallel manipulators and closeness to singularity," *J. Mech. Robot.* **1**(1), 011011 (2008).
20. P. A. Voglewede and I. Ebert-Uphoff, "Measuring "Closeness" to Singularities for Parallel Manipulators," *Proceedings of the 2004 IEEE International Conference on Robotics and Automation*, New Orleans, LA, USA (2004) pp. 4539–4544.
21. P. A. Voglewede and I. Ebert-Uphoff, "Overarching framework for measuring closeness to singularities of parallel manipulators," *IEEE Trans. Robot.* **21**(6), 1037–1045 (2005).

22. F. Pierrot, "Parallel Mechanisms and Redundancy," *Proceedings of the 1st International Colloquium, Collaborative Research Centre 562*, Braunschweig, Germany (2002) pp. 261–277.
23. F. M. Dimentberg, *The Screw Calculus and Its Applications in Mechanics* (Foreign Technology Division, Springfield, VA, USA, 1968) 155 pp.
24. M. G. Mohamed and J. Duffy, "A direct determination of the instantaneous kinematics of fully parallel robot manipulators," *ASME J. Mech. Transm. Autom. Des.* **107**(2), 226–229 (1985).
25. D. Zlatanov, I. A. Bonev and C. M. Gosselin, "Constraint Singularities of Parallel Mechanisms," *Proceedings of the IEEE International Conference on Robotics and Automation*, Washington, DC, USA (2002) pp. 496–502.
26. P. Laryushkin, V. Glazunov and S. Demidov, "Singularity Analysis of 3-DOF Translational Parallel Manipulator," *Advances on Theory and Practice of Robots and Manipulators. Proceedings of ROMANSY 2014 XX CISM-IFToMM Symposium on Theory and Practice of Robots and Manipulators*, Moscow, Russia (2014) pp. 47–54.
27. I. Bonev and C. Gosselin, "Singularity Loci of Planar Parallel Manipulators with Revolute Joints," *Proceedings of the 2nd Workshop on Computational Kinematics*, Seoul, South Korea (2001) pp. 1–11.